Eur. Phys. J. D **24**, 105–109 (2003)
DOI: 10.1140/epjd/e2003-00187-4

THE EUROPEAN PHYSICAL JOURNAL D

Chirality, defects, and disorder in gold clusters

I.L. Garzón[1,a], M.R. Beltrán[2], G. González[2], I. Gutíerrez-González[1], K. Michaelian[1], J.A. Reyes-Nava[1], and J.I. Rodríguez-Hernández[2]

[1] Instituto de Física, Universidad Nacional Autónoma de México, Apartado Postal 20-364, México D.F., 01000 México
[2] Instituto de Investigaciones en Materiales, Universidad Nacional Autónoma de México, Apartado Postal 70-360, México D.F., 01000 México

Received 10 September 2002
Published online 3 July 2003 –

Abstract. Theoretical and experimental information on the shape and morphology of bare and passivated gold clusters is fundamental to predict and understand their electronic, optical, and other physical and chemical properties. An effective theoretical approach to determine the lowest-energy configuration (global minimum) and the structures of low energy isomers (local minima) of clusters is to combine genetic algorithms and many-body potentials (to perform global structural optimizations), and first-principles density functional theory (to confirm the stability and energy ordering of the local minima). The main trend emerging from structural optimizations of bare Au clusters in the size range of 12−212 atoms indicates that many topologically interesting low-symmetry, disordered structures exist with energy near or below the lowest-energy ordered isomer. For example, chiral structures have been obtained as the lowest-energy isomers of bare Au_{28} and Au_{55} clusters, whereas in the size-range of 75−212 atoms, defective Marks decahedral structures are nearly degenerate in energy with the ordered symmetrical isomers. For methylthiol-passivated gold nanoclusters [$Au_{28}(SCH_3)_{16}$ and $Au_{38}(SCH_3)_{24}$], density functional structural relaxations have shown that the ligands are not only playing the role of passivating molecules, but their effect is strong enough to distort the metal cluster structure. In this work, a theoretical approach to characterize and quantify chirality in clusters, based on the Hausdorff chirality measure, is described. After calculating the index of chirality in bare and passivated gold clusters, it is found that the thiol monolayer induces or increases the degree of chirality of the metallic core. We also report simulated high-resolution transmission electron microscopy (HRTEM) images which show that defects in decahedral gold nanoclusters, with size between 1−2 nm, can be detected using currently available experimental HRTEM techniques.

PACS. 36.40.-c Atomic and molecular clusters – 36.40.Mr Spectroscopy and geometrical structure of clusters

1 Introduction

Extensive theoretical studies on the geometrical structures of the most stable isomers of bare and passivated gold clusters have shown that these systems have interesting and perhaps unique peculiarities. For example, in the small size regime, quantum mechanical calculations of neutral Au_n ($n \leq 6$) clusters indicate that the lowest-energy configurations correspond to planar (two-dimensional) structures [1]. These results have been attributed to the strong non-additivity of the many-body forces existing in small noble metal clusters [2,3]. In the intermediate size range ($n = 12-55$), global structural optimizations of Au_n clusters have shown that many topologically interesting low-symmetry, disordered structures exist with energy near or below the lowest-energy ordered isomer [4–10]. For these clusters, it was shown that the physical origin of the cluster distortion is related to a mechanism for strain relief that lowers the cluster energy [9,10]. More recently, it has been found using density functional (DFT) calculations that in gold nanoclusters (Au_n, n = 75, 101, 146, 192, and 212), defective decahedral structures are nearly degenerate in energy with the highly symmetrical Marks decahedron isomer [11].

In other studies on thiol-passivated gold clusters, we have shown that the effect of a methylthiol monolayer is strong enough to distort the metallic core of an initially ordered gold cluster. This result was obtained by performing unconstrained DFT structural relaxations on $Au_{28}(SCH_3)_{16}$ and $Au_{38}(SCH_3)_{24}$, using different cluster-monolayer configurations [12–14]. The large cluster distortion upon passivation can be explained through the strong

[a] e-mail: garzon@fisica.unam.mx

covalent (directional) interaction existing between the sulfur atom of the passivating thiol and the gold atoms in the metallic cluster core [15].

Although most of the results mentioned above have been confirmed and extended by other theoretical groups (existence of planar structures in small neutral and charged Au clusters [16–19]; degeneracy in energy of amorphous or disordered isomers with ordered structures for intermediate size gold clusters [20–22]; and strong distortion of the metal core structure due to the interaction with thiol molecules in passivated Au clusters [23,24]), relatively few experimental works have been dedicated to detect and characterize cluster structures with low symmetry or asymmetrical geometries. Nevertheless, during the last few years some interesting experimental results have been reported on the existence of disordered gold clusters. In one of them, intense optical activity has been measured in passivated Au clusters in the size range of 20−40 atoms, suggesting that the structure of the metal cluster is inherently chiral [25]. In another study on larger Au clusters of 2−4 nm in size, complex and defective structures have been detected using X-ray diffraction (XRD) [26].

In order to provide additional theoretical information to further motivate experimental work in investigating physical and chemical properties of Au clusters with disordered or defective structures, we describe in the present paper a methodology to characterize and quantify the index of chirality of clusters with asymmetrical geometries. We also report image simulations of high-resolution transmission electronic microscopy (HRTEM), which show that defective decahedral structures can be detected in gold particles between 1−2 nm. Section 2 contains a description of the methodology to calculate the index of chirality in clusters and the results for bare and passivated Au clusters of different size, as well as their comparison with other nanostructures. In Section 3, we report results on simulated HRTEM images of defective Au nanoclusters. A summary of this work is given in Section 4.

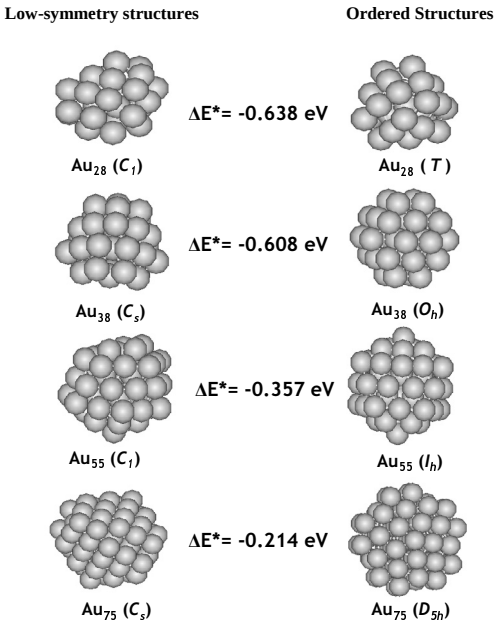

Fig. 1. Lowest-energy structures of disordered (low-symmetry) and ordered gold clusters. For each size, it is shown the difference in total energy between both structures, calculated using DFT within the generalized-gradient approximation. For additional details on these calculations, see references [9,14]. The low-symmetry structures are more stable for the four cluster sizes displayed.

2 Chirality in clusters

Since a common characteristic of the most stable isomers of bare and passivated gold clusters of intermediate sizes ($n = 12-75$ atoms) is the existence of structural disorder (Fig. 1 shows the geometries of the lowest-energy structures, disordered and ordered, for some bare gold clusters in this size range), it is important to describe and understand the type of structural patterns existing in such systems [10]. An initial attempt [5] to quantify the amount and type of local disorder existing in amorphouslike structures of the Au_{55} cluster was performed using the common-neighbor analysis [27–29]. In that case, it was found that the distorted multilayer icosahedral order is the most abundant in the lowest-energy amorphouslike isomers of Au_{55} [5].

More recently, we have initiated a more detailed investigation not only to analyze the type of disorder existing in gold clusters, but to determine the existence of chirality in such systems, and quantify this property, by assigning an index of chirality that allows the comparison among clusters [14]. This approach has the advantage of providing useful insights to interpret recent experimental results that have detected intense optical activity in passivated gold clusters, suggesting that the metallic core of these systems is inherently chiral [25]. In the following, we describe the theoretical approach to quantify chirality in clusters, providing additional details that complete the description given in a preliminary report [14].

Chirality is a geometrical property of clusters that does not depend on its physical or chemical manifestations, therefore, it is possible to quantify this property without any reference to experimental measurements, but only using the inherent structural symmetry of the system. Several methods have been proposed in the past to quantify molecular chirality [30,31], however, a unification of chirality measures has recently been suggested [30]. An extensive review of chirality measures, reveals that the one which measures to what extent two enantiomorphs differ from one another has wider application [32,33]. Specifically, the Hausdorff chirality measure (HCM) has emerged as the general method of choice to quantify molecular chirality [32,33]. In this approach, the degree of chirality is obtained by calculating the maximal overlap between two enantiomorphs, the actual cluster and its mirror image. The overlap can be calculated using the Hausdorff distance (HD) between the sets of atomic coordinates that represent the actual cluster and its mirror image. By rotating and translating the mirror image with respect to the original cluster, the optimal overlap can be obtained.

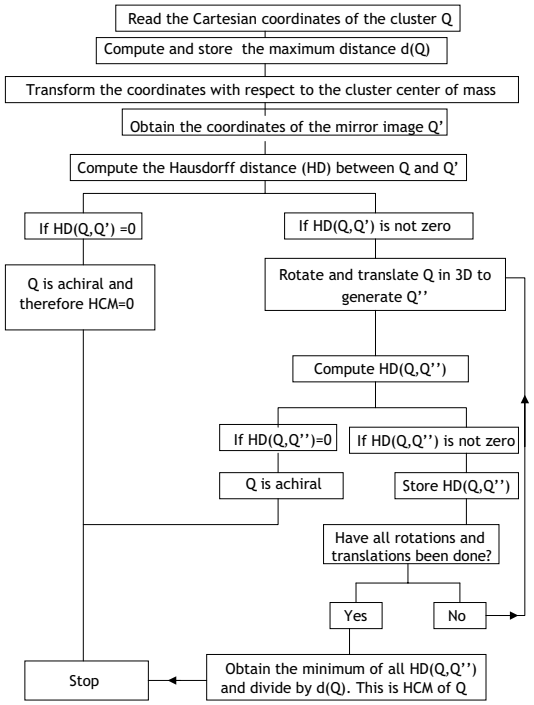

Fig. 2. Flow-chart that shows the procedure to calculate the Hausdorff chirality measure (HCM) from the Cartesian coordinates of the optimized clusters.

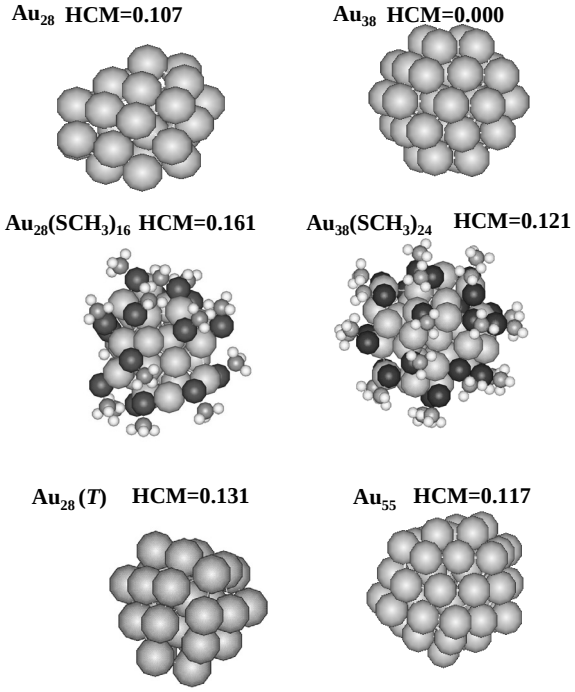

Fig. 3. Structures of bare and methylthiol-passivated chiral gold clusters. The structures of the passivated clusters correspond to the lowest-energy configurations obtained from DFT optimizations within the generalized-gradient approximation, using several cluster-monolayer configurations. See references [12–14] for more information on these calculations. The structures of the bare clusters in the top panels were distorted upon passivation with the thiol molecules. The darker spheres correspond to sulfur atoms. The index of chirality (HCM) for each gold cluster is also shown.

The mathematical expression for HD between two arbitrary sets is given in references [32,33]. A more intuitive definition of HD, also given in references [32,33], establishes that the Hausdorff distance $h(Q, Q')$ between the sets Q and Q' can be defined as the smallest number $\delta = h(Q, Q')$ that has the following properties: (a) a sphere of radius δ centered at any point of Q contains at least one point of Q' and (b) a sphere of radius δ centered at any point of Q' contains at least one point of Q.

There are several advantages in using HCM to quantify chirality: first, it is a continuous and similarly invariant function of the cluster shape, second, it is zero only if the cluster is achiral, and finally, its numerical implementation to study large clusters in a three-dimensional space is straightforward [32,33]. Figure 2 shows a flow-chart that describes the numerical procedure to calculate HCM from the Cartesian coordinates of any cluster. We have used the optimized geometries of several bare and methylthiol-passivated gold clusters to obtain their index of chirality HCM. In Figure 3, we present the structures and the HCM values of several chiral gold clusters. The bare Au_{28} and Au_{38} clusters displayed at the top panels of Figure 3 have HCM values lower than those corresponding to the distorted metallic core obtained upon passivation shown in the middle panels. This result indicates that the passivation effect is strong enough to increase the chirality of a bare cluster (Au_{28}) or even more interestingly, it could induce chirality in an initially achiral cluster (Au_{38}).

The HCM values calculated for bare and passivated clusters have been compared with the corresponding values of other nanostructures like chiral D_2-C_{78} and D_2-C_{84} fullerenes. It results that the chiral gold clusters displayed in Figure 3 are as chiral as those fullerenes [14]. However, it remains to be seen if the clusters with different chirality can be detected experimentally. In this respect, circular dichroism spectroscopy seems to be an appropriate technique to study the above effect, as has been suggested from the optical activity measurements in passivated gold-glutathione cluster compounds [25].

3 Defects in decahedral gold clusters

To explore the possible detection of defects in gold decahedral structures with size 1−2 nm, we have simulated HRTEM images using our calculated cluster geometries and parameters corresponding to commercial microscopes like JEOL 4000EX and JEOL 2010. To confirm the calculated images two programs have been used with the same outcome [34,35]. Both programs are based on the multislice approximation [36], which is appropriate for the study of finite systems (clusters) [36]. The simulated images presented here were obtained using the following parameters: Accelerating voltage = 400 keV, spherical aberration coefficient C_s = 1.06 mm, beam semi-convergence = 0.6 (mrad), defocus spread = 9 nm,

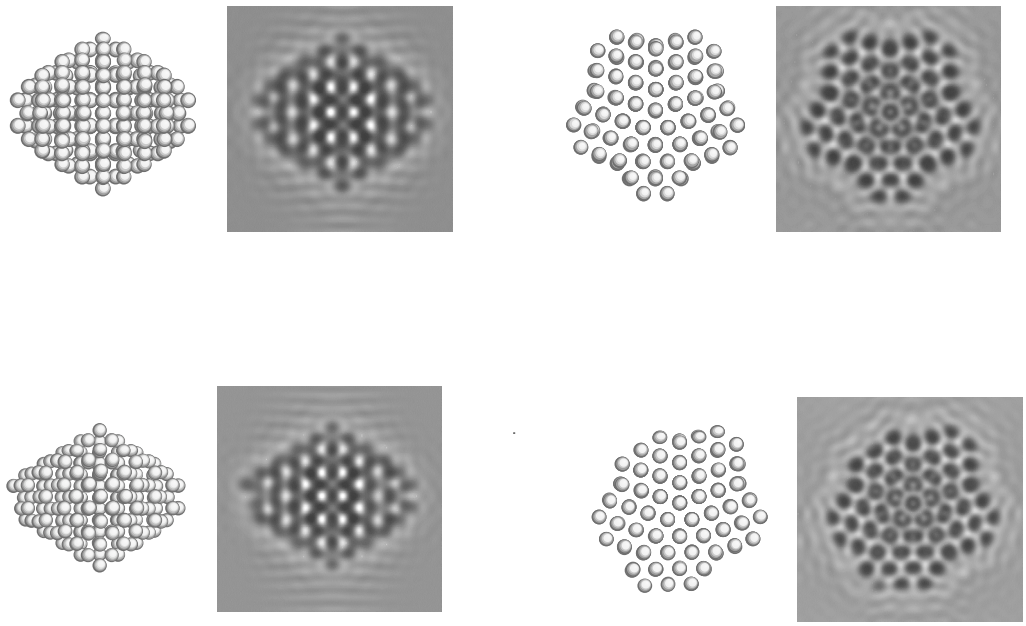

Fig. 4. Two views of the Au_{212} structure for both, the geometrical model and the calculated HRTEM image for (top panels) perfect Marks decahedra, and (bottom panels) defective Marks decahedra.

objective aperture = 26 nm^{-1}, and Scherzer defocus = –48 nm, corresponding to a JEOL 4000EX microscope. These optimal microscope conditions lead to a point to point resolution of 0.16 nm, which is less than one half of the interatomic gold distance.

Figure 4 shows the simulated images of both perfect and defective Marks decahedral structures with 212 atoms which are nearly degenerate in energy. On the left hand side (first column), side views of both perfect (top panel) and defective (bottom panel) clusters are displayed, showing two-fold symmetry axes. In this orientation, there is not point to point matching with the original structures because the projected atoms partially overlap, nevertheless, the defective image (bottom panel) has few extra atoms on the left hand side (probably difficult to be observed under real experimental conditions). On the other hand, in the right hand column both the perfect (top panel) and defective (bottom panel) images are oriented specifically under maximum overlap, generating intercolumnar atom distances larger than 1.6 nm, that make possible a structural identification. Clearly, if the clusters are conveniently oriented, it is possible to detect the differences between perfect and defective structures. The defects found in larger clusters (>100 atoms) are mainly at the cluster surface, the inner core being practically unchanged from the ordered case [11]. It is important to note that in some cases where the defects are only local, the information from the real images may depend largely on the orientation chosen. This is due to the interatomic projected distances which have to be of the order of the microscope maximum resolution $\sim$ 1.6 nm. This condition can only be achieved for a small number of cluster orientations and it would be particularly difficult to see in small clusters due to the lack of contrast.

4 Summary

Systematic cluster structure optimizations, using state of the art theoretical methods, have shown that the most stable (lowest-energy) structures of bare gold clusters present interesting peculiarities (planar, chiral, and defective configurations) as a function of cluster size. Chirality is an inherent geometrical property of clusters that can be quantified using the Hausdorff chirality measure and the Cartesian coordinates of the relaxed clusters. The main results on chirality in gold clusters indicate that the lowest-energy structures of bare Au_{28} and Au_{55} are chiral, whereas thiol-passivation induces or increase chirality in intermediate size gold clusters.

For bare gold clusters with size 1−2 nm, it has been found that defective Marks decahedral structures are nearly degenerate in energy with the perfect Marks decahedral isomer. In addition, we predict that the defects on the cluster surface can be experimentally detected, using currently available HRTEM techniques.

It is important to remark that the above peculiarities of the structural properties of gold clusters do not result from kinetic or temperature effects, but are due to special bonding mechanisms involving Au atoms (strong non-additivity in the many-body forces, short-range interaction, relativistic effects, and *d*-electrons contribution) that generate a complex potential energy surface. These factors would indicate that small (nano) gold corresponds to a special type of material. In summary, the theoretical results reported in this paper provide useful predictions and information that complements the experimental work, which for gold clusters up to 2 nm in size is still scarce.

This work was supported by DGAPA-UNAM under Project IN104402 and DGSCA-UNAM Supercomputing Center.

References

1. G. Bravo-Pérez, I.L. Garzón, O. Novaro, J. Mol. Struct. (Theochem) **493**, 225 (1999)
2. I.L. Garzón, I.G. Kaplan, R. Santamaria, O. Novaro, J. Chem. Phys. **109**, 2176 (1998)
3. G. Bravo-Pérez, I.L. Garzón, O. Novaro, Chem. Phys. Lett. **313**, 655 (1999)
4. I.L. Garzón, J. Jellinek, Z. Phys. D **26**, 316 (1993)
5. I.L. Garzón, A. Posada-Amarillas, Phys. Rev. B **54**, 11796 (1996)
6. I.L. Garzón, K. Michaelian, M.R. Beltrán, A. Posada-Amarillas, P. Ordejón, E. Artacho, D. Sánchez-Portal, J.M. Soler, Phys. Rev. Lett. **81**, 1600 (1998)
7. I.L. Garzón, K. Michaelian, M.R. Beltrán, A. Posada-Amarillas, P. Ordejón, E. Artacho, D. Sánchez-Portal, J.M. Soler, Eur. Phys. J. D **9**, 211 (1999)
8. K. Michaelian, N. Rendón, I.L. Garzón, Phys. Rev. B **60**, 2000 (1999)
9. J.M. Soler, M.R. Beltrán, K. Michaelian, I.L. Garzón, P. Ordejón, D. Sánchez-Portal, E. Artacho, Phys. Rev. B **61**, 5771 (2000)
10. J.M. Soler, I.L. Garzón, J.D. Joannopoulos, Solid State Commun. **117**, 621 (2001)
11. M.R. Beltrán *et al.*, to be published
12. I.L. Garzón, C. Rovira, K. Michaelian, M.R. Beltrán, P. Ordejón, J. Junquera, D. Sánchez-Portal, E. Artacho, J.M. Soler, Phys. Rev. Lett. **85**, 5250 (2000)
13. I.L. Garzón, E. Artacho, M.R. Beltrán, A. García, J. Junquera, P. Ordejón, C. Rovira, D. Sánchez-Portal, J.M. Soler, Nanotechnology **12**, 126 (2001)
14. I.L. Garzón, J.A. Reyes-Nava, J.I. Rodríguez-Hernández, I. Sigal, M.R. Beltrán, K. Michaelian, Phys. Rev. B **66**, 073403 (2002)
15. G. Bravo-Pérez, I.L. Garzón, J. Mol. Struct. (Theochem) **619**, 79 (2002)
16. H. Häkkinen, U. Landman, Phys. Rev. B **62**, R2287 (2000)
17. S. Gilb, P. Weis, F. Furche, R. Ahlrichs, M.M. Kappes, J. Chem. Phys. **116**, 4094 (2002)
18. H. Häkkinen, M. Moseler, U. Landman, Phys. Rev. Lett. **89**, 033401 (2002)
19. V. Bonačić-Koutecký, J. Burda, R. Mitrić, M. Ge, G. Zampella, P. Fantucci, J. Chem. Phys. **117**, 3120 (2002)
20. T.X. Li, S.Y. Yin, Y.L. Yi, B.L. Wang, G.H. Wang, J.J. Zhao, Phys. Lett. A **267**, 403 (2000)
21. S. Darby, T.V. Mortiner-Jones, R.L. Johnston, C. Roberts, J. Chem. Phys. **116**, 1536 (2002)
22. J. Wang, G. Wang, J. Zhao, Phys. Rev. B **66**, 035418 (2002)
23. D. Krüger, H. Fuchs, R. Rosseau, D. Marx, M. Parrinello, J. Chem. Phys. **115**, 4776 (2001)
24. J.A. Larsson, M. Nolan, J.C. Greer, J. Phys. Chem. B **106**, 5931 (2002)
25. G.T. Schaaff, R.L. Whetten, J. Phys. Chem. B **104**, 2630 (2000)
26. D. Zanchet, B.D. Hall, D. Ugarte, J. Phys. Chem. B **104**, 11013 (2000)
27. E. Blaisten-Barojas, H.C. Andersen, Surf. Sci. **156**, 548 (1985)
28. J.D. Honeycutt, H.C. Andersen, J. Phys. Chem. **91**, 4950 (1987)
29. D. Faken, H. Jónsson, Comput. Mater. Sci. **2**, 279 (1994)
30. N. Weinberg, K. Mislow, J. Math. Chem. **17**, 35 (1995)
31. M. Solymosi, R.J. Low, M. Grayson, M.P. Neal, J. Chem. Phys. **116**, 9875 (2002)
32. A.B. Buda, K. Mislow, J. Am. Chem. Soc. **114**, 6006 (1992)
33. A.B. Buda, T. Auf der Heyde, K. Mislow, Angew. Chem. Int. Ed. Engl. **31**, 989 (1992)
34. P. Stadelmann, Ultramicroscopy **21**, 131 (1987)
35. A. Gómez, L.M. Beltrán, Rev. Latin. Metalur. Mater. **21**, 46 (2001)
36. J.M. Cowley, A.F Moodie, Acta Crystallogr. **10**, 609 (1957); **12**, 353 (1959)